Supplemental material for Bagherkhani and Baghlani, "Enhancing curvature mode shape method for structural damage severity estimation by means of distributed genetic algorithm", *Engineering Optimization*, 2020.

S1. Damage detection in beam structures

In Table 1, various damage scenarios in the damaged one-bay beam are introduced. In addition, the natural frequencies of the first four modes of the intact and damaged beams are reported. Figure 1 shows the first four mode shapes of an intact one-bay beam.

Table 1. Natural frequencies of the intact and damaged one-bay beam under different damage scenarios.

	Element number	Damage severity (%)	Natural frequency			
			Mode 1	Mode 2	Mode 3	Mode 4
Intact	-	-	13.09	52.36	117.81	209.46
Scenario 1	10	90	9.50	51.85	97.42	203.48
Scenario 2	7, 14	65, 65	11.62	45.98	117.31	192.28
Scenario 3	4, 10, 11, 17	70, 50, 50, 70	11.37	44.57	91.94	187.13

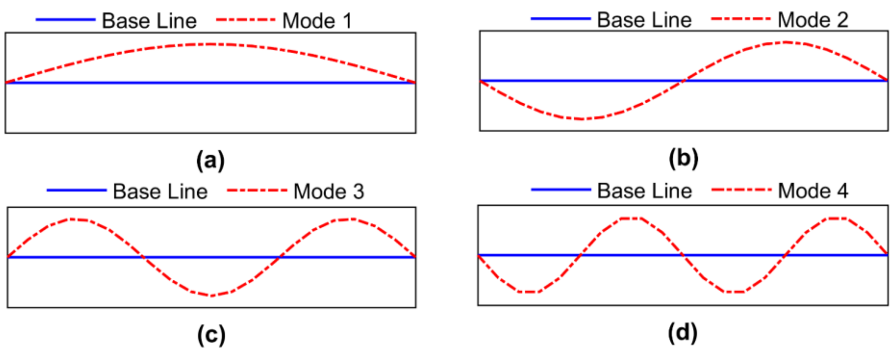

Figure 1. Mode shapes of one-bay beam: (a) first mode, (b) second mode, (c) third mode, and (d) fourth mode.

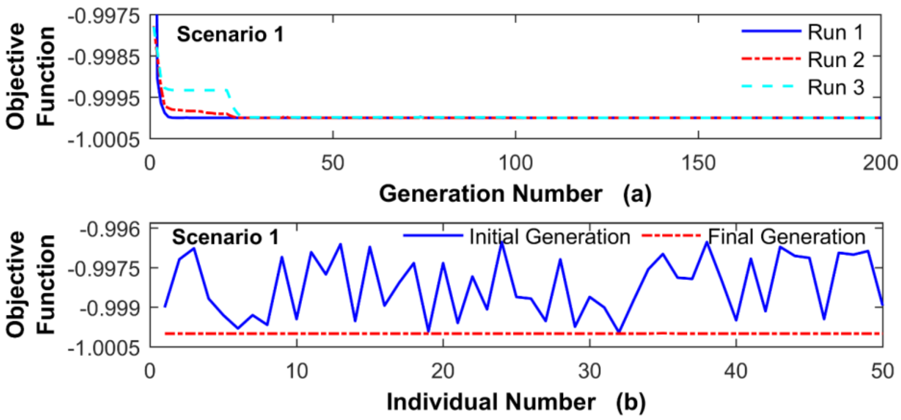

Figure 2. Convergence of DGA for one-bay beam: (a) objective function in successive generation, and (b) values of objective function in population of the first and last generation.

In Figure 2a, the convergence trend of the objective function in successive generations of Scenario 1 for one-bay beam is shown. As can be seen, the value of objective function in three different runs finally converges to value of -1. Figure 2b shows the values of objective function for population of the first and last generations of Run 1, which indicates the same fitness of individuals in the last generation. In Table 2, various damage scenarios in the damaged two-bay beam are introduced.

Table 2. Natural frequencies of the intact and damaged two-bay beam under different damage scenarios.

	Element number	Damage severity (%)	Natural frequency			
			Mode 1	Mode 2	Mode 3	Mode 4
Intact	-	-	13.09	20.45	52.36	66.27
Scenario 1	10, 30	90, 90	9.50	16.90	51.85	63.66
Scenario 2	10, 20, 21, 30	50, 90, 90, 50	12.44	15.18	51.52	56.98

S2. Damage detection in frame structures

The first four mode shapes of the intact one-bay frame are shown in Figure 3. In Table 3 various damage scenarios in the damaged one-bay frame are introduced. Moreover, the natural frequencies of the first four modes of the intact and damaged frames are reported. 3D-plots of curvature difference for first mode of one-bay frame under three damage scenarios are presented in Figure 4. Figure 5a shows the convergence of objective function in successive generations of Scenario 1 for one-bay frame. In Figure 5b, the values of objective function for population of the first and last generations associated with Run 1 are given.

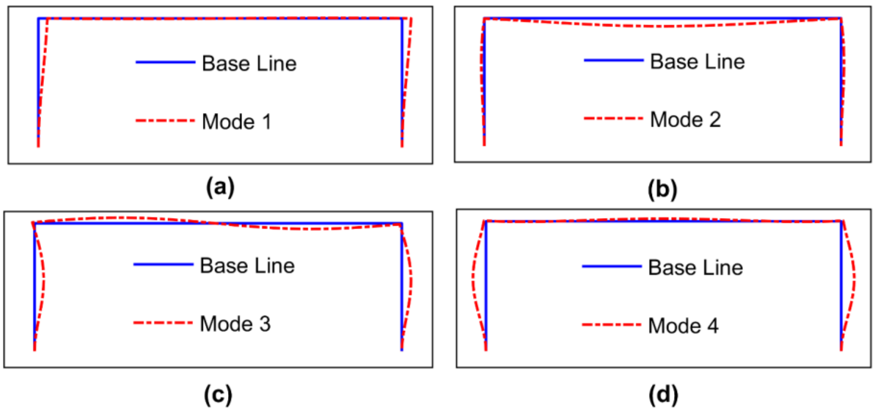

Figure 3. Mode shapes of one-bay frame: (a) first mode, (b) second mode, (c) third mode, and (d) fourth mode.

Table 3. Natural frequencies of the intact and damaged one-bay frame under different damage scenarios.

	Element number	Damage severity (%)	Natural frequency			
			Mode 1	Mode 2	Mode 3	Mode 4
Intact	-	-	36.21	90.59	225.04	247.66
Scenario 1	29	90	36.20	77.10	224.36	238.22
Scenario 2	8, 49	70, 70	35.97	89.64	215.51	232.81
Scenario 3	10, 29, 47	80, 65, 50	36.18	84.51	209.77	231.28

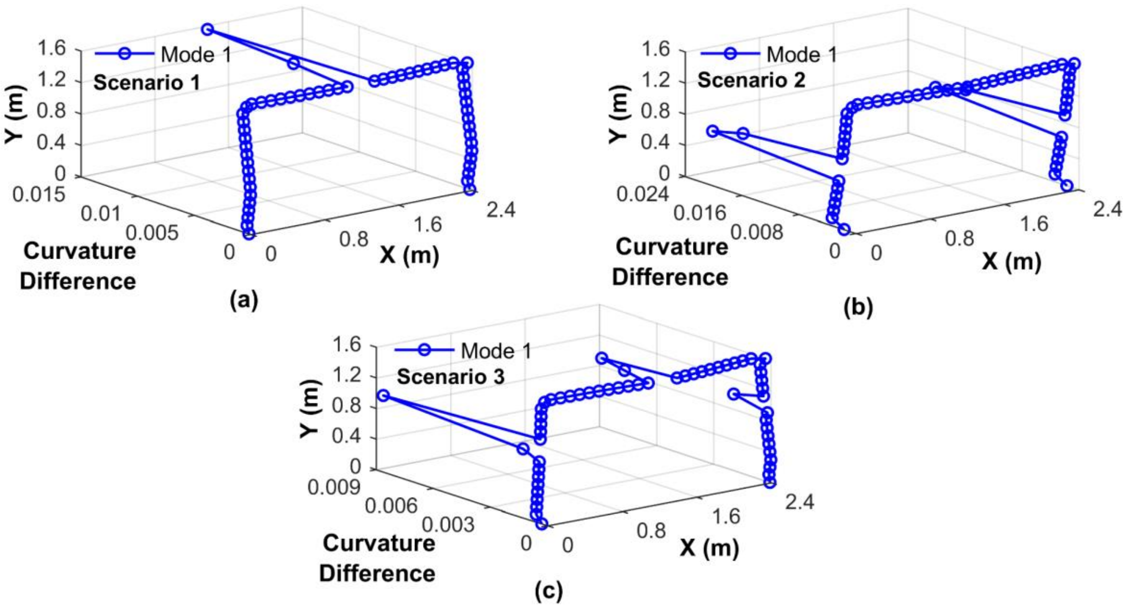

Figure 4. 3D-plots of curvature difference of one-bay frame in first mode: (a) Scenario 1, (b) Scenario 2, and (c) Scenario 3.

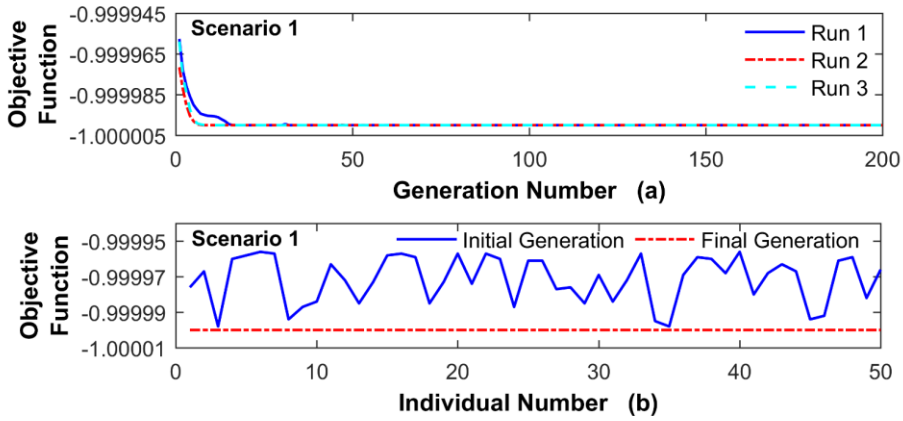

Figure 5. Convergence of DGA for one-bay frame: (a) objective function in successive generation, and (b) values of objective function in population of the first and last generation.

Various damage scenarios in the damaged two-bay frame are introduced in Table 4. Figure 6 shows 3D-plots of curvature difference for first mode of two-bay frame under four damage scenarios.

Table 4. Natural frequencies of the intact and damaged two-bay frame under different damage scenarios.

	Element number	Damage severity (%)	Natural frequency			
			Mode 1	Mode 2	Mode 3	Mode 4
Intact	-	-	16.15	52.98	80.99	96.76
Scenario 1	10	50	16.15	52.94	80.93	96.69
Scenario 2	25, 65	90, 90	16.09	52.79	74.54	92.61
Scenario 3	10, 25, 175	90, 70, 80	16.03	52.66	79.61	94.78
Scenario 4	25, 65, 104, 137, 175	65, 80, 60, 70, 55	16.08	52.90	76.96	94.38

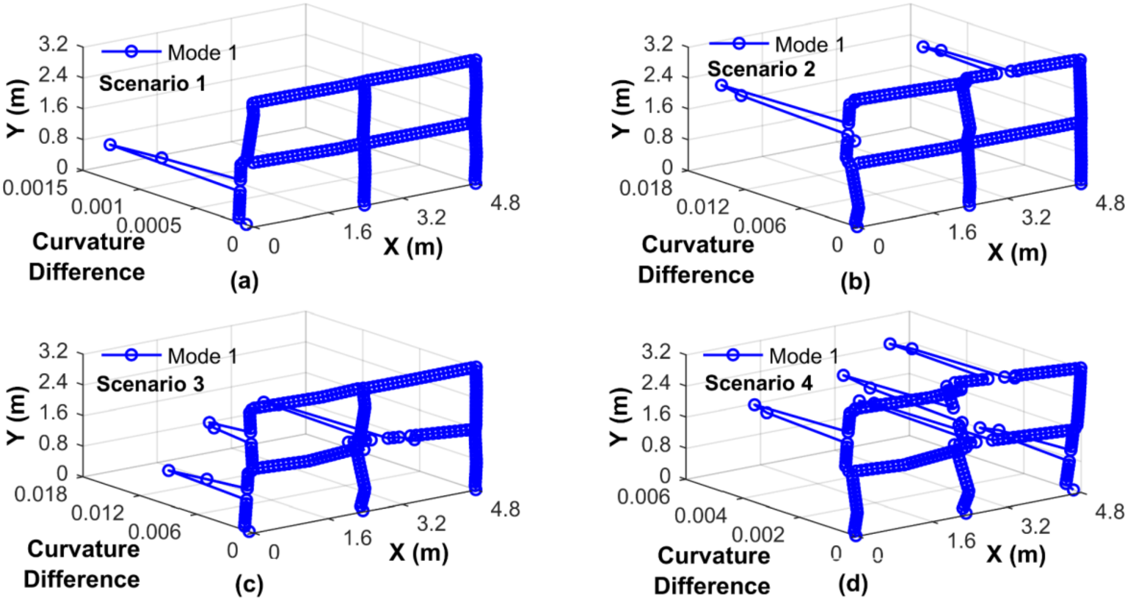

Figure 6. 3D-plots of curvature difference of two-bay frame in first mode: (a) Scenario 1, (b) Scenario 2, (c) Scenario 3, and (d) Scenario 4.

S3. The effect of noisy data

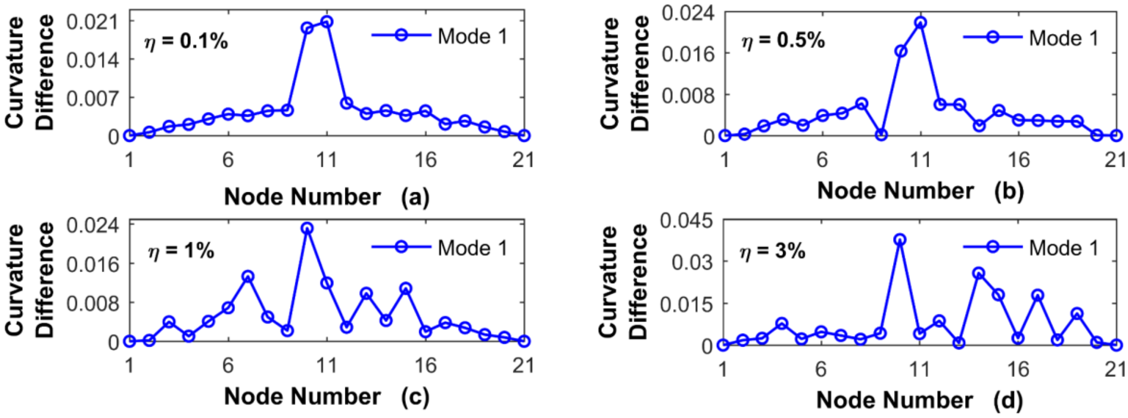

Figure 7. Curvature difference of one-bay beam in Scenario 1 for various noise levels: (a) 0.1%, (b) 0.5%, (c) 1%, and (d) 3%.

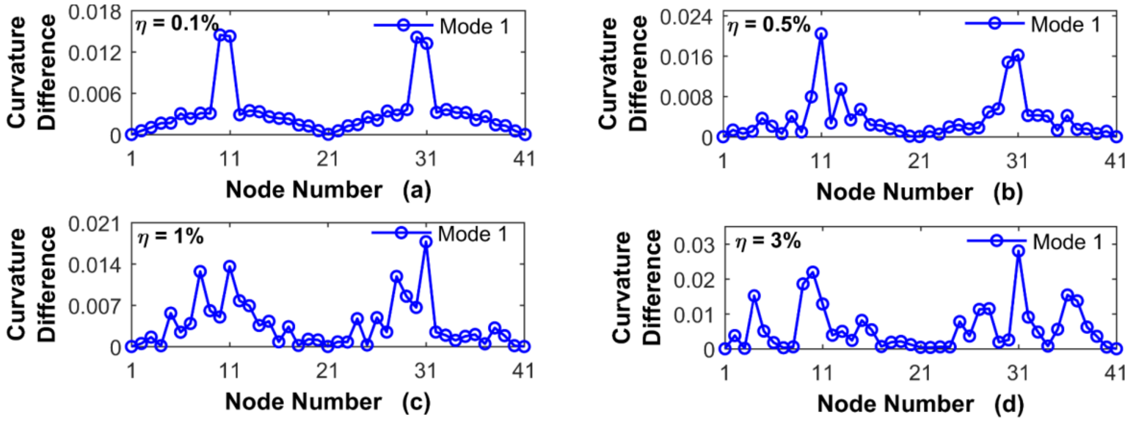

Figure 8. Curvature difference of two-bay beam in Scenario 1 for various noise levels: (a) 0.1%, (b) 0.5%, (c) 1%, and (d) 3%.

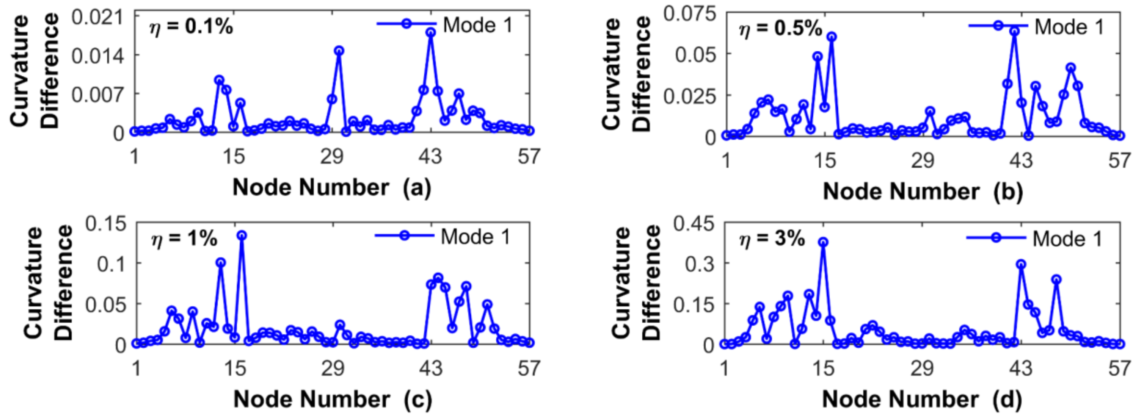

Figure 9. Curvature difference of one-bay frame in Scenario 1 for various noise levels: (a) 0.1%, (b) 0.5%, (c) 1%, and (d) 3%.

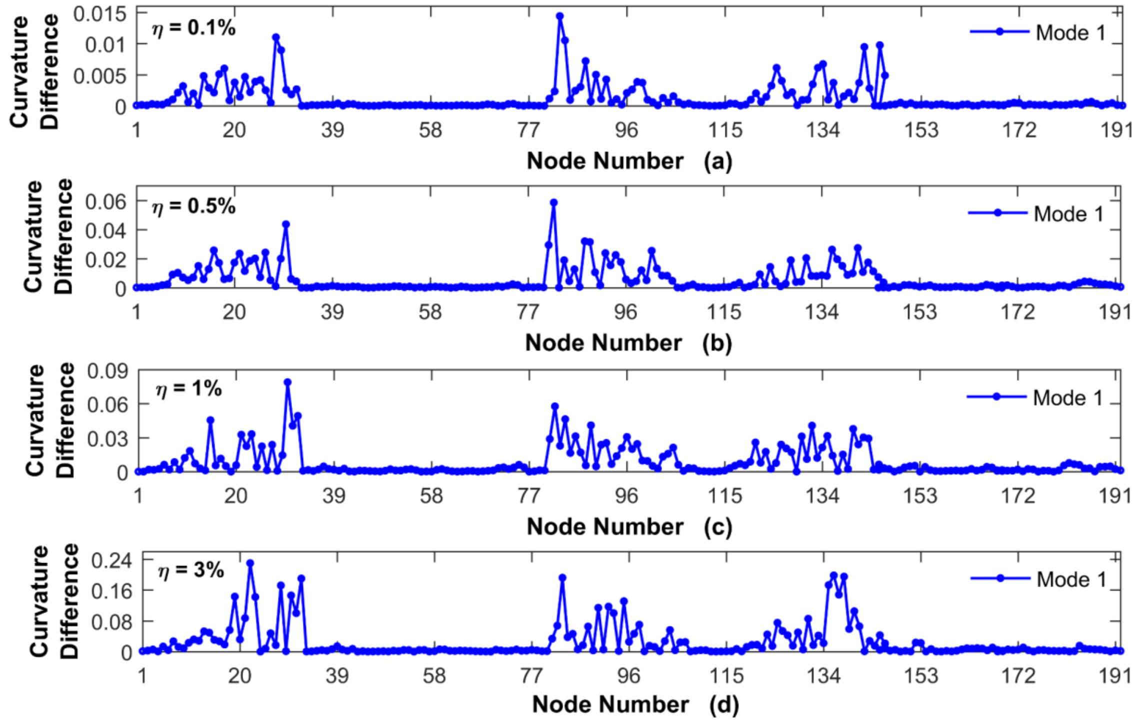

Figure 10. Curvature difference of two-bay frame in Scenario 1 for various noise levels: (a) 0.1%, (b) 0.5%, (c) 1%, and (d) 3%.

Curvature difference between the first mode shapes of the intact and damaged structures at the nodes is presented in Figures 7 and 10 for Scenario 1 of damage scenarios.

S4. Damage detection in experimental beam

In Table 5 the natural frequencies of the first three modes of intact and damaged structures are reported. In Figure 11 the first mode shapes of structure related to intact and damaged beam in two cases of experimental results and FE model are presented.

In Figure 12a the convergence trends of objective function in successive generations for three runs of experimental beam are shown. Moreover, the values of objective function for population of the first and last generations of Run 1 are shown in Figure 12b.

Table 5. Natural frequencies of the intact and damaged experimental beam.

	Natural Frequency		
	Mode 1	**Mode 2**	**Mode 3**
Intact (Experimental)	85.726	238.572	467.694
Damaged (Experimental)	83.984	235.792	462.712
Intact (FEM)	87.232	240.462	471.424
Damaged (FEM)	75.779	226.975	432.361

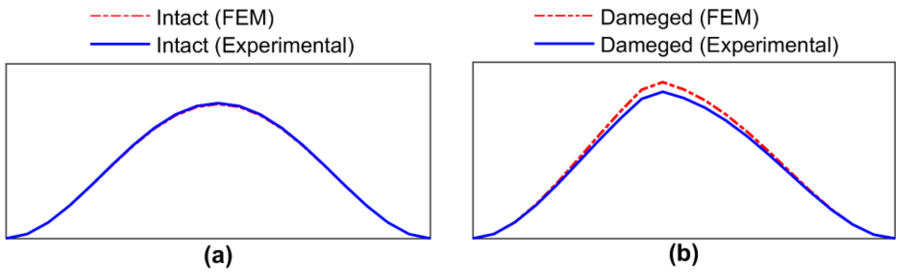

Figure 11. First mode shape of experimental beam: (a) intact beam, and (b) damaged beam.

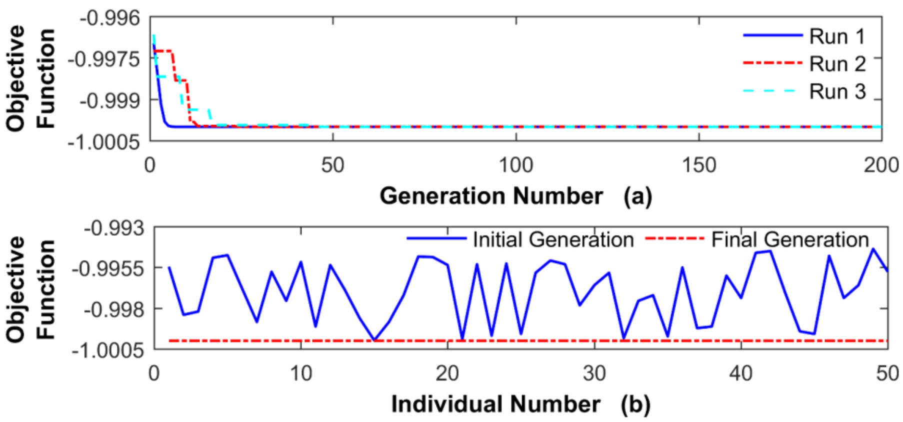

Figure 12. Convergence of DGA for experimental beam: (a) objective function in successive generation, and (b) values of objective function in population of the first and last generation.